# A Molecular Mechanism of Enantiorecognition of Tertiary Alcohols by Carboxylesterases

Erik Henke,[a] Uwe T. Bornscheuer,[b] Rolf D. Schmid,[a] and Jürgen Pleiss*[a]

*Carboxylesterases containing the sequence motif GGGX catalyze the hydrolysis of esters of chiral tertiary alcohols, albeit with only low to moderate enantioselectivity, for three model substrates (linalyl acetate, methyl-1-pentin-1-yl acetate, 2-phenyl-3-butin-2-yl acetate). In order to understand the molecular mechanism of enantiorecognition and to improve enantioselectivity for this interesting substrate class, the interaction of both enantiomers with the substrate binding sites of acetylcholinesterases and* p*-nitrobenzyl esterase from* Bacillus subtilis *was modeled and correlated to experimental enantioselectivity. For all substrate–enzyme pairs, enantiopreference and ranking by enantioselectivity could be predicted by the model. In* p*-nitrobenzyl esterase, one of the key residues in determining enantioselectivity was G105: exchange of this amino acid for an alanine residue led to a sixfold increase of enantioselectivity (*E = *19) towards 2-phenyl-3-butin-2-yl acetate. However, the effect of this mutation is specific: the same mutant had the opposite enantiopreference towards the substrate linalyl acetate. Thus, depending on the substrate structure, the same mutant has either increased enantioselectivity or opposite enantiopreference compared to the wild-type enzyme.*

**KEYWORDS:**

enantioselectivity · enzyme catalysis · molecular modeling · protein design · tertiary alcohols

## Introduction

One of the key questions in understanding structure–function relationships of enzymes is how these molecules distinguish between the two enantiomers of a chiral substrate. Lipases (E.C. 3.1.1.3) and esterases (E.C. 3.1.1.1) are widely used as enantioselective catalysts by organic chemists.[1, 2] Although lipases and esterases show no general sequence similarity, they share a common architecture, the $\alpha/\beta$ hydrolase fold,[3] which consists of eight central $\beta$ strands surrounded by $\alpha$ helices. Their catalytic mechanism is also identical: the catalytic machinery consists of an amino acid triad (serine, histidine, and aspartate or glutamate), with a serine residue acting as a nucleophile and attacking the carbonyl carbon atom of the substrate ester, while a histidine residue acts as an amphiphile and catalyzes the withdrawal of the alcohol moiety by transferring a proton onto the ester oxygen atom.[4]

Most lipases and esterases show enantiorecognition of chiral alcohols or carboxylic acids, but enantioselectivity is often not high enough for industrial applications. In order to use these enzymes in chiral synthesis, their enantioselectivity can be further increased by substrate engineering,[5] solvent variation,[6] immobilization,[7] modification of parameters like temperature,[8] pH value,[9] and pressure,[10] or by modification of the enzyme's structure. Several attempts to vary enantioselectivity of esterases and lipases by directed evolution[11–13] and by rational protein engineering have been successful.[14, 15] The latter method also yields insight into the molecular mechanism of enantiorecognition. X-ray structures of several lipases and esterases complexed with chiral substrate-analogous inhibitors are available. This information has made it possible to understand the structural basis of an empirical rule for predicting the enantiopreference of an enzyme towards esters of secondary alcohols from the structure of the substrate alone.[16, 17] However, for other substrates like small primary alcohols and triacylglycerols such a universal rule for all lipases is not applicable.[18] In general, enantiopreference depends on the details of the structure of both the substrate and the enzyme. Methods involving computer-aided molecular modeling have been successfully used to study these interactions and identify determinants of enantioselectivity.[19–21]

The synthesis of optically pure substances with a quaternary stereogenic center is still a challenge, not only in biocatalysis but also in classical stereoselective synthesis.[22] A promising route to an optically pure compound with a quaternary stereogenic center is through esterase-catalyzed kinetic resolution of chiral tertiary alcohols. While carboxylester hydrolases are widely used for the synthesis of optically pure secondary alcohols and to a

[a] *Dr. J. Pleiss, Dr. E. Henke, Prof. R. D. Schmid*
*Institute of Technical Biochemistry*
*University of Stuttgart*
*Allmandring 31*
*70569 Stuttgart (Germany)*
*Fax: (+49) 711-685-3196*
*E-mail: itbjpl@po.uni-stuttgart.de*

[b] *Prof. Dr. U. T. Bornscheuer*
*Institute of Chemistry and Biochemistry*
*Greifswald University*
*Soldmannstrasse 16*
*17487 Greifswald (Germany)*

 **DOI: 10.1002/cbic.200200518**  

smaller extent also for the resolution of primary alcohols and carboxylic acids,[1, 23] there are only a few examples of utilization of these enzymes for the hydrolysis of esters of tertiary alcohols (TAEs). Tertiary alcohols (TAs) are generally not accepted as substrates by carboxylester hydrolases of commercial interest, probably as a result of the sterically demanding structure of these compounds.[24, 25] The only hydrolases that are active towards this class of substrates are characterized by a highly conserved GGG(A)X motif,[26] which is located in the active site and contributes to the formation of the so-called oxyanion hole.[27] This binding pocket stabilizes the oxyanion in the tetrahedral intermediate formed during the catalytic cycle of ester hydrolysis.[28] GGG(A)X-type hydrolases are mostly carboxylesterases and often have eukaryotic origin. In contrast, most bacterial lipases and esterases, which are preferentially used in biotransformation, do not have this GGG(A)X motif but instead have a GX pattern. The two groups, GGG(A)X and GX hydrolases, differ significantly in the structure of the catalytic site.[27] Recently, our finding that GGG(A)X-type hydrolases are able to hydrolyze esters of tertiary alcohols was confirmed by the discovery of a GGG(A)X-type esterase from the hyperthermophilic archaeon *Pyrobaculum calidifontis* that hydrolyzes *tert*-butyl acetate.[29]

To understand the molecular mechanism of enantiorecognition of tertiary alcohols by carboxylesterases, the enantioselectivity of several enzymes towards esters of chiral tertiary alcohols were investigated in vitro and in silico. A refined computer-based model made it possible to explain the experimentally observed enantioselectivity and to predict the effect of mutations.

## Results

### Enantioselectivity

Seven GGG(A)X-type carboxylesterases were tested for their enantioselectivity towards chiral TAEs: two preparations of pig liver esterase (PLE), acetylcholine esterases from the banded krait (*Bungarus fasciatus*, bAChE), electric eel (*Electrophorus electricus*, eeAChE), and human (hAChE), lipase from *Candida rugosa* (CRL) and a recombinant *p*-nitrobenzyl esterase from *Bacillus subtilis* (BsubpNBE). Hydrolytic reactions were performed with a pH stat. Enzyme-catalyzed hydrolysis of three model substrates (Scheme 1) occurred with only low to moderate enantioselectivity (Table 1). Linalyl acetate **1** was converted by all hydrolases uniformly with enantioselectivities $E$ of less than 2 ($E$ = ratio of $R/S$), CRL did not show any enantiorecognition at all. Interestingly, the two commercial PLE preparations (Chirazyme E1 and E2, Roche, Mannheim) displayed opposite enantiopreference, albeit at a very low level of enantioselectivity. For 3-methyl-1-pentin-3-yl acetate **2**, the hydrolases differed in the degree of enantiorecognition: enantioselectivities between $E = 3$ and $E = 7$ were obtained with PLE and the AChEs. Towards this substrate, CRL showed lower enantioselectivity ($E = 2$) than PLE or the AChEs, while BsubpNBE was nonselective ($E = 1$). Considerable differences in enantioselectivity were obtained by using 2-phenyl-3-butin-2-yl acetate **3** as substrate: the AChEs converted **3** with the highest enantioselectivity ($E = 3 - 10$), while PLE E1 ($E =$ 1.3) had very low and CRL ($E = 1$) no enantioselectivity. PLE E2 was significantly more selective ($E = 5$) than the E1 preparation. BsubpNBE ($E = 3$) accepted **3** with higher enantioselectivity than substrates **1** and **2**.

The various AChEs showed considerably different enantioselectivity towards substrates **2** and **3**, particularly substrate **3**. While eeAChE and hAChE converted both substrates with enantioselectivities of $E = 4$ and $E = 3$, respectively, bAChE was more selective ($E = 7$ and $E = 10$ towards **2** and **3**, respectively).

### Modeling of AChEs

The difference between the enantioselectivity of eeAChE and that of bAChE was modeled by comparing the interactions between the two substrate enantiomers and the binding site of the esterases. While the structures of eeAChE (Protein Data Base (PDB) entry 1C2B)[30] and hAChE (PDB entry 2CLJ, homology model)[31] are available, the structure of bAChE has not yet been determined. bAChE has sequence identities of 55%, 57%, and 65% to eeAChE, hAChE, and to AChE from *Torpedo californica* (tcAChE), respectively. Consequently, the structure of bAChE was modeled based on the tcAChE structure (PDB entries 1QIK and 1CFJ).[32] While the overall sequence similarity of eeAChE and bAChE is moderate, the binding pocket itself is highly conserved. The sequence in this region is 95% identical within a sphere of 10 Å around the catalytic histidine residue ($His_{act}$) and the structures differ only slightly. This high conservation explains the similar catalytic activities and identical enantiopreference of these enzymes. The major difference between the two AChE structures is the orientation of the side chain of W86, which in the bAChE binding pocket is shifted by 1.5 Å towards the catalytic center compared to its position in eeAChE.

Models of the complexes of both enantiomers of **3** with eeAChE and bAChE showed significant differences in the stability of the complexes under simulation conditions. While the preferred (*R*)-**3** enantiomer fitted well into the binding pocket of both enzymes, the (*S*)-**3** enantiomer faced strong repulsive forces in bAChE as a result of an interaction of the phenyl substituent of the substrate with residue W86 (Figure 1). This repulsive interaction was not observed in the eeAChE-(*S*)-**3** complex, which explains the experimentally observed higher enantioselectivity of bAChE.

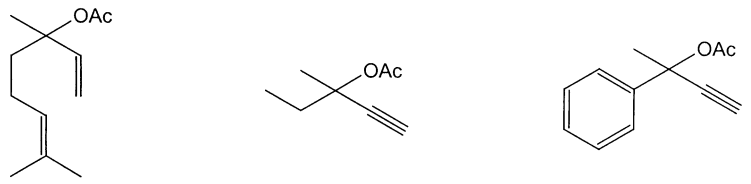


Linalyl acetate
**1**

3-Methyl-1-pentin-3-yl acetate
**2**

2-Phenyl-3-butin-2-yl acetate
**3**

***Scheme 1.*** *Model substrates used in the experiments and molecular modeling described herein.*

  

**Table 1.** *Enantioselectivity of GGG(A)X-type hydrolases towards TAEs.*[a]

| Enzyme | Substrate (Amount [μmol]) | Time | Conversion [%] | $E$[e] |
|---|---|---|---|---|
| PLE E1, 10 mg, 390 U[b] | **1** (50) | 8 h | 48 | 1.5 (*R*) |
| | **2** (50) | 2 h | 53 | 4 (*S*) |
| | **3** (200), 440 U | 32 min | 50 | 1.3 (*R*) |
| PLE E2, 10 mg, 270 U[b] | **1** (50) | 4 h | 42 | 1.7 (*S*) |
| | **2** (50) | 2 h | 69 | 4 (*S*) |
| | **3** (200) | 21 min | 50 | 5 (*R*) |
| bAChE, 100 U[c] | **1** (50) | 48 h | 6 | 1.1 (*S*) |
| | **2** (50) | 4 h | 25 | 7 (*S*) |
| | **3** (50) | 1 h | 48 | 10 (*R*) |
| eeAChE, 100 U[b] | **1** (50) | 48 h | 10 | 1.5 (*S*) |
| | **2** (50) | 24 h | 26 | 4 (*S*) |
| | **3** (50) | 4 h | 50 | 4 (*R*) |
| hAChE, 37.5 U[c] | **1** (50) | 48 h | 5 | 1.1 (*S*) |
| | **2** (50) | 24 h | 17 | 3 (*S*) |
| | **3** (50) | 4 h | 39 | 3 (*R*) |
| CLEC-CRL, 10 mg | **1** (50) | 8 h | 23 | 1.0 |
| | **2** (50) | 2 h | 56 | 2 (*S*) |
| | **3** (50) | 30 min | 77 | 1.0 |
| BsubpNBE WT, 10 mg, 350 U[d] | **1** (200) | 38 min | 50 | 1.7 (*R*) |
| | **2** (200) | 49 min | 50 | 1.0 |
| | **3** (200) | 20 min | 50 | 3 (*R*) |
| BsubpNBE A400I, 10 mg, 230 U[d] | **1** (200) | 27 min | 50 | 2 (*R*) |
| | **2** (200) | 70 min | 50 | 1.0 |
| | **3** (200) | 22 min | 50 | 2 (*R*) |
| BsubpNBE G105A, 80 mg, 350 U[d] | **1** (200) | 60 min | 54 | 4 (*S*) |
| | **2** (200) | 150 min | 50 | 1.3 (*S*) |
| | **3** (200) | 22 min | 50 | 19 (*R*) |

[a] Reactions were carried out at pH 7.5 and 40 °C (AChEs: 25 °C). Enantiomeric excesses and conversions were determined by GC on a chiral column. Enantioselectivity was calculated according to the procedure described by Chen et al.[33] The enantioselectivities shown are averages of values calculated at different time points in at least two individual experiments. Conversions are examples from one single experiment. The error margin of the determined enantioselectivities is within ±10%. [b] According to the manufacturer. [c] Ellman assay for acetylthiocholine. [d] Towards *p*-NPA. [e] Configuration of the preferred enantiomer is indicated in parentheses.

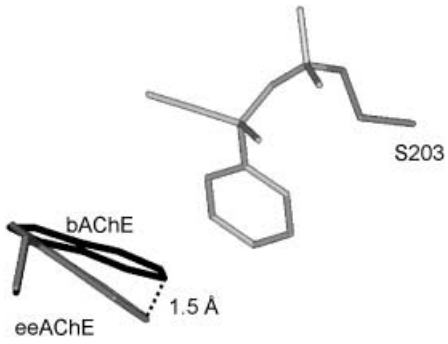


***Figure 1.*** *Orientation of W86 in the binding pockets of eeAChE (gray) and bAChE (black). The active S203 (gray) of eeAChE and the covalently bound disfavored enantiomer (S)-**3** (light gray) are shown. The W86 side chain of bAChE is 1.5 Å closer to the substrate than that of eeAChE as a result of interactions with its neighbor, M85 (not shown).*

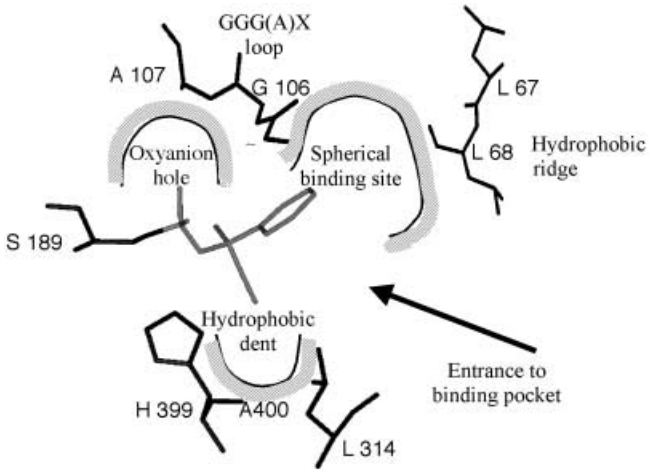


***Figure 2.*** *Binding of (S)-**3** to BsubpNBE; the distinct binding pockets are indicated.*

### Protein engineering of BsubpNBE

A similar modeling strategy was applied to BsubpNBE to explain enantiopreference and enantioselectivity, and to design mutants with improved enantioselectivity. The alcohol binding site of BsubpNBE is hydrophobic and nearly spherical at the bottom (Figure 2). Two opposite walls consisting of the GGAX loop and A400 limit this sphere. This is a feature that distinguishes the GGG(A)X-type hydrolases from the GX-type hydrolases, in which the corresponding residues form a steep wall that prevents the access of tertiary alcohols by blocking the binding of a third substituent in this direction. This sphere in BsubpNBE opens towards a large, hydrophobic gorge (Figure 3). A 4-Å pocket, the hydrophobic dent, composed of F313, L314, and A400 is also present. Towards the acyl binding tunnel this dent is terminated by $His_{act}$ (H399). The active site is almost open to solvent, except

  

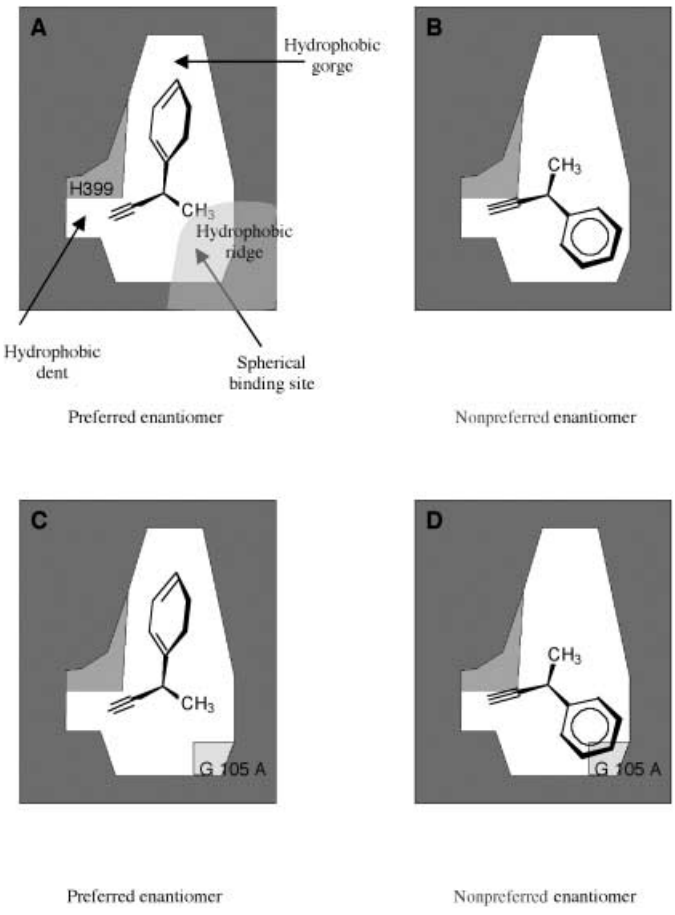


***Figure 3.*** *Binding pocket of wild-type BsubpNBE (a, b) and mutant G105A (c, d) complexed with (R)-**3** (a, c) and (S)-**3** (b, d). $His_{act}$ (H399) and the hydrophobic ridge (L67 and L68) are shown in (a).*

for a hydrophobic ridge-shaped loop (L67, L68) blocking the entrance in front of the GGAX loop (Figure 2).

For both enantiomers of **3**, the medium-sized ethinyl substituent is located in the hydrophobic dent. The bulky phenyl substituent is bound differently: for the preferred (*R*)-**3** enantiomer, the phenyl ring points into the hydrophobic gorge (Figure 3A) and for the (*S*)-**3** into the spherical hydrophobic pocket near the hydrophobic ridge (Figure 3B). Both complexes were stable and they have a similar conformation, which explains the low enantioselectivity of BsubpNBE towards this substrate.

To validate this model, mutants with improved enantioselectivity towards **3** were predicted. To increase enantioselectivity, a potential mutation should prevent binding of the enantiomer not preferred by the enzyme or improve binding of the preferred enantiomer. Two promising residues for mutagenesis, A400 and G105, were identified. Replacing one of these amino acids by residues with a more space-demanding side chain was expected to complicate binding of (*S*)-**3** by interaction of the residue side chain with the phenyl substituent of the substrate. Molecular dynamics (MD) simulations of BsubpNBE G105A indeed showed a rejection of the (*S*)-**3** phenyl substituent and consequently less favorable binding of the (*S*)-enantiomer (Figure 4, B1 and C1). The proximity of G105 to the active S189 meant that an exchange of G105 with a residue even more bulky than alanine was not possible without reducing the catalytic activity. In contrast, substitution of A400 by isoleucine, leucine, valine, or phenylalanine had no effect on the (*S*)-enantiomer. The sizes of the isoleucine, leucine, and valine side chains were not sufficient to interfere with the phenyl substituent of the substrate. The phenylalanine side chain, however, did not orient towards the binding pocket but pointed towards other aromatic residues nearby.

When the two enantiomers of **1** were docked to mutant G105A, modeling studies predicted a switch from *R* to *S* preference. The computer model showed an increased interference of the small methyl substituent of the (*R*)-enantiomer with the enlarged A105 residue, but no change in interaction with the (*S*)-enantiomer. This outcome is in contrast to the results of experiments with **3**, where the less-preferable (*S*)-enantiomer interacts with A105. The (*R*)-enantiomers of the two substrates interact with the enzyme differently: for (*R*)-**1**, the largest alkyl substituent is oriented into the hydrophobic dent; as a result of binding of this substituent to the wall of the hydrophobic dent, the methyl substituent comes closer to the A105 residue than observed with (*R*)-**3** (Figure 4).

To validate simulation results, mutants BsubpNBE A400I, G105A, and double mutant A400I/G105A were generated and expressed in *Escherichia coli*. Activity and enantioselectivity were determined and compared to those of the wild-type enzyme. While mutation A400I barely changed expression and activity, G105A reduced activity of BsubpNBE towards *p*-nitrophenyl acetate (pNPA) to 10% of the wild-type activity. The double mutant showed no observable activity. As predicted by molecular modeling, enantioselectivity towards **3** was not changed by A400I, while mutation G105A led to a sixfold increase of enantioselectivity from $E = 3$ (BsubpNBE WT; WT = wild type) to $E = 19$ (BsubpNBE G105A; Table 1). Mutant G105A also showed the predicted inversion of enantiopreference towards **1**: BsubpNBE WT preferred hydrolysis of the (*R*)-enantiomer with low enantioselectivity ($E = 1.7$), while the mutant BsubpNBE G105A favored the (*S*)-enantiomer ($E = 4$). Towards substrate **2**, for which BsubpNBE WT has been shown to be completely unselective, mutant G105A shows very low but significant enantioselectivity ($E = 1.3$) and prefers the (*S*)-enantiomer.

Determination of enantioselectivity comprises two sources of error. The enantiomeric excess (*ee*) can be experimentally determined with high precision (±2%) by gas chromatographic analysis. However, because of the approximations in the formula used to calculate enantioselectivity from *ee* values,[33] the error margin for *E* values is about 10%. Although the value of *E* is given with a 10% accuracy, the change from nonselective to low enantioselectivity can be identified with a much higher degree of reliability.

In the MD simulations the enantiomer not preferred by the enzyme is pushed out of the optimal binding orientation as a consequence of repulsive interaction. This process leads to an increase in the distance between the active histidine residue and the ester oxygen atom. Thus, the distance between the

  

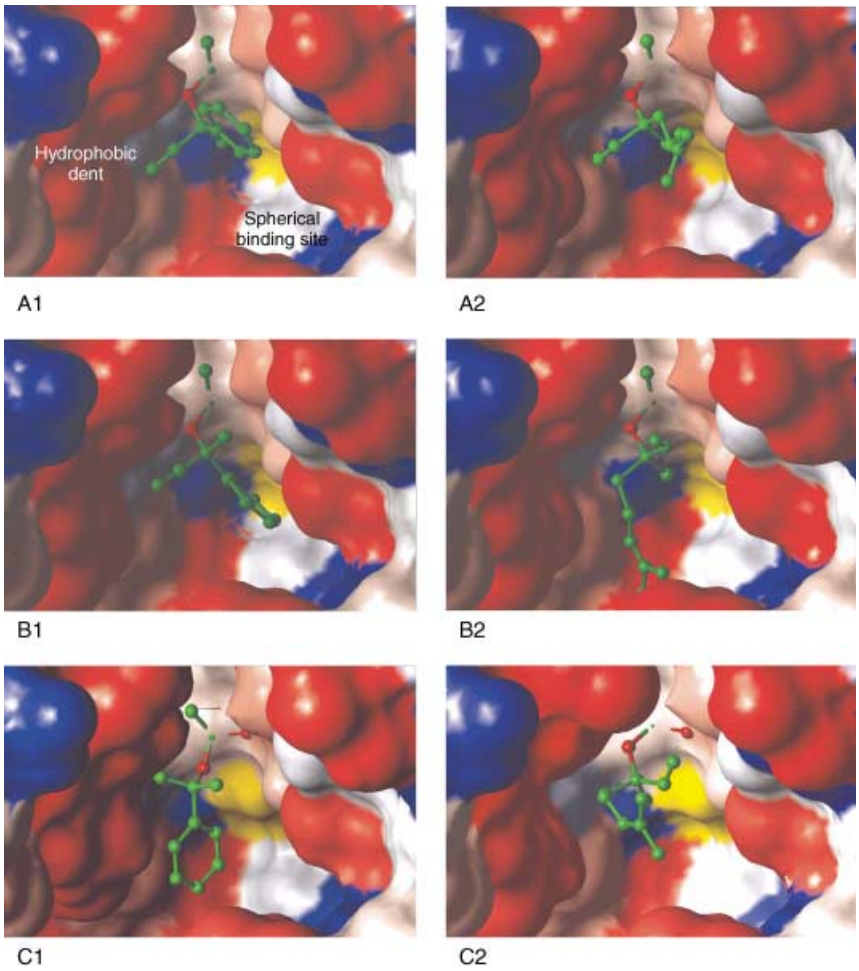


***Figure 4.*** *Binding of substrates **2** and **3** in the binding pocket of BsubpNBE WT and BsubpNBE G105A. The protein surface is colored according to the hydrophobicity of the residues. G105 in BsubpNBE WT and A105 in the mutant are colored yellow. For better clarity, hydrogen atoms are not shown. A) WT with preferred substrate enantiomers (A1: (S)-**3**; A2: (R)-**1**). B) WT with nonpreferred substrate enantiomers (B1: (S)-**3**; B2: (R)-**1**). C) Mutant G105A with nonpreferred substrate enantiomers (C1: (S)-**3**; C2: (S)-**1**).*

protonated $N_\varepsilon$ atom of $His_{act}$ and the ester oxygen atom $O_{ester}$ [$d(N_\varepsilon H - O_{ester})$] was taken as a geometrical probe to quantify effects on enantioselectivity (Scheme 2). A small distance $d(N_\varepsilon H - O_{ester})$ is necessary to ensure stabilization of the substrate

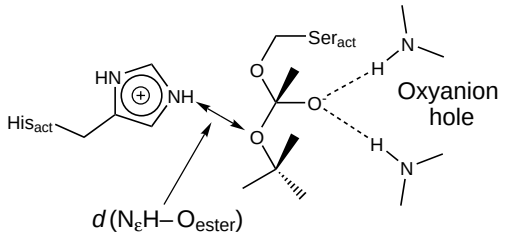


***Scheme 2.*** *Tetrahedral intermediate: The substrate ester is covalently bound to the $Ser_{act}$ residue. The anionic intermediate formed is stabilized by hydrogen bonds to the oxyanion-hole residues. The complex shown was used for modeling studies. The distance between the $N_\varepsilon$ proton and the oxygen atom of the ester bond ($d(N_\varepsilon H - O_{ester})$) is indicated. The difference between the distances observed in models of the enzyme complexes with each of the enantiomers ($\Delta d(N_\varepsilon H - O_{ester})$) can be used as a parameter to indicate the enantioselectivity.*

complex and proton transfer during the catalytic cycle. The difference $\Delta d(N_\varepsilon H - O_{ester})$ observed between the modeled complexes with the preferred and less preferable enantiomer is a quantitative measure of the difference in activity towards the two enantiomers, and thus the difference in the experimentally determined enantioselectivity. Indeed, experimental *E* values correlate well with $\Delta d(N_\varepsilon H - O_{ester})$ as derived from the computer model (Figure 5), and enantioselectivity can be predicted directly from MD simulations.

## Discussion

### Modeling enantioselectivity towards TAEs

Manual docking, relaxation by MD simulation, and geometric analysis were used to establish a model for understanding and predicting enantioselectivity towards TAEs. The model identifies a geometric probe, $\Delta d(N_\varepsilon H - O_{ester})$, which is correlated to experimentally determined enantiopreference and enantioselectivity. A similar model has previously been applied to explain enantioselectivities of lipases towards chiral substrates like triacylglycerols and secondary alcohols.[10, 15, 19, 20, 34] The results for secondary alcohols are in accordance with complementary methods that model enantioselectivity in hydrolase-catalyzed reactions by evaluating the free energy of enzyme – substrate complexes.[21, 35]

### Small changes in structure lead to small changes in enantioselectivity

Intuitively, one would expect that homologous enzymes have identical enantiopreference, as

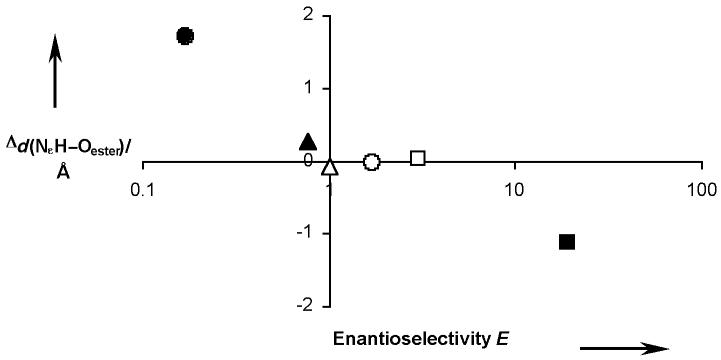


***Figure 5.*** *Correlation of modeling data ($\Delta$d($N_\varepsilon H - O_{ester}$)) and experimental results (E = ratio R/S); enantioselectivity of wild-type BsubpNBE (open symbols) and the mutant BsubpNBE G105A (solid symbols) towards linalyl acetate (**1**; circles), 3-methyl-1-pentin-3-yl acetate (**2**; triangles), and 2-phenyl-3-butin-2-yl acetate (**3**; squares)*

  

was observed for AChEs from different organisms, where differences in sequence led to changes in *E* values but not to a reversal of enantiopreference. However, this rule cannot be generalized, as has been shown previously for two homologous lipases from *Rhizopus oryzae* and *Rhizomucor miehei* in which small structural changes led to opposite stereopreference towards triacylglycerols.[19] A switch of enantiopreference between two similar enzymes could also explain our observation that two commercial PLE preparations (chirazyme E-1 and E-2) have opposite enantiopreference towards **1**. This difference is most probably caused by the different compositions of the PLE fractions since it has been demonstrated that commercial PLE preparations frequently contain several hydrolytic enzymes[36] and isoenzymes.[37] The presence of these enzymes may result not only in an opposite enantiopreference of two preparations, but also in an apparent enantioselectivity that is much lower than for the individual purified isoenzyme.[38]

#### Switch in enantiopreference

Changing the enantiopreference of a biocatalyst is still a challenge. In asymmetric organic synthesis a switch in the handedness of the reaction can be achieved by exchange of the chiral auxiliary with its enantiomeric counterpart (that is, by switching from L- to D-tartrate in the Sharpless epoxidation[39]). In biocatalysis, this inversion of the enantiotopic surrounding corresponds to an exchange of the natural L-enzyme with a chemically synthesized D-enzyme, as has been demonstrated for HIV protease.[40] Interestingly, a switch in the enantiopreference of a biocatalyst can sometimes be obtained with only small changes of sequence and structure. A single mutation in BsubpNBE led to a switch in enantioselectivity towards substrate **1** from (*R*)-preference of the wild-type enzyme to (*S*)-preference of the mutant G105A. The model predicted that the orientation of the substrate would change as a result of the mutation: the now-preferred (*S*)-enantiomer binds through the smallest (methyl) substituent to the hydrophobic gorge, while in the wild-type enzyme the largest substituent is oriented into this huge binding pocket. In contrast, substrate **3** binds in a similar orientation to both the wild-type and the mutant enzyme. Thus, small changes in the shape of the binding site have opposite effects on different substrates. Therefore, a generally valid empirical rule for predicting the preferred enantiomer only from the structure of the substrate is not feasible for tertiary alcohols. This fact distinguishes enantiorecognition of tertiary and secondary alcohols from one another since secondary alcohols all bind in a similar conformation to the lipase binding site and thus enantiopreference can be predicted by a simple and general rule.[16, 17]

Changes of enantiopreference as a result of point mutations in the substrate binding site have also been observed for lipases,[15] phosphotriesterases,[41] lactate dehydrogenases,[42] and alcohol dehydrogenases.[43] Thus, our results support the general idea that enantiopreference is not an inherent property of an enzyme but can be tuned by protein engineering. A switch of enantiopreference by point mutations was also achieved by directed evolution experiments.[13, 44] Since mutations were far away from the substrate binding site, their effect on enantiorecognition is still obscure. These long-range effects indicate that mutations might have further effects, like changing the overall structure of the protein or its dynamics.[45]

The successful change in enantiopreference and enantioselectivity achieved by the single mutation G105A in BsubpNBE demonstrates that this site is a major determinant in enantiorecognition since it imposes sterical restraints on the shape of the substrate near its stereocenter. This observation is further underlined by comparing the effect of two single mutations to that of a double mutation. Although A400 and G105 are situated at opposite sides of the binding site, their effect on activity is highly synergic. While the mutation A400I had no effect on enzyme activity and mutant G105A still had 10% of the wild-type activity, a combination of both mutations completely inactivated the enzyme ($<0.1$% wild-type activity). The relevance of G105 is also underlined by the observation that, as the first residue of the GGG(A)X motif,[27] it is highly conserved in all carboxylesterases. The only exception is an $\alpha$-esterase from *Drosophila buzzatii*, in which G105 is replaced by a proline residue.[46] The mutation G105P in BsubpNBE resulted in a substantial loss of activity ($<1$% wild-type activity, data not shown), which also indicates that the enzyme does not tolerate considerable changes in this region.

#### Enhancing enantioselectivity

While mutation G105A in BsubpNBE led to a switch in enantiopreferences towards substrate **1**, enantiopreference towards substrate **3** did not switch. Instead, the model predicted a considerable increase in enantioselectivity towards substrate **3**, which was experimentally confirmed. An enantioselectivity of $E=19$ is an appropriate starting point for further improvement of enantioselectivity by standard methods like substrate engineering, solvent modification, enzyme immobilization, or temperature and pH changes, to achieve a level of enantioselectivity suitable for industrial applications.

## Conclusion

Our findings show that the effect of replacing an amino acid side chain in an enzyme cannot be generalized for all substrates, but has to be considered for each substrate–enzyme pair independently. Since the conformations of the two enantiomers in the binding site depend on the details of the structures of both substrate and enzyme, the effect of a mutation in the enzyme is specific to the substrate involved. Thus, the same mutation G105A can lead to a switch of enantiopreference (substrate **1**), generation of enantiorecognition (substrate **2**), or sixfold increase in enantioselectivity (substrate **3**). The effects of mutations depend on differences in the interaction of the enzyme with the two substrate enantiomers: if the mutant primarily blocks the binding of the disfavoured enantiomer, enantioselectivity is increased, if it blocks binding of the preferred enantiomer enantioselectivity is decreased or even reversed.

  

Thus, enantiorecognition by esterases can be explained on a molecular level by careful investigation of the interactions between enzyme and substrate. From a quantitative model of enantioselectivity, mutants with useful properties in relation to individual substrates can be predicted.

## Experimental section

**General**: Chemicals were purchased from Fluka (Buchs, Switzerland) or Sigma (Deisenhofen, Germany) at the highest purity available. PLE (Chirazyme E1 and E2) were purchased from Roche (Mannheim, Germany), CRL-CLEC from Altus (Cambridge, MA), and eeAChE from Sigma. NMR spectroscopy experiments were performed on a Bruker 500-MHz device.

**Cloning of hydrolases**: Genomic DNA from *Bacillus subtilis* DSM 402 was isolated according to a standard protocol.[47] BsubpNBE was cloned by amplification of the previously described open reading frame[48] from the genomic DNA by using primers 5′-ACT ACT ACT ACT CAT ATG ACT CAT CAA ATA GTA ACG – 3′ and 5′-CTA CTA CTA CTA GGA TCC TTC TCC TTT TGA AGG-3′. The PCR product was digested by using restriction endonucleases *BamH*I and *Nde*I and was ligated into an expression vector to yield the plasmid pG-BsubpNBE.WT.

**Protein expression system**: *p*-Nitrobenzyl esterase from *Bacillus subtilis* and variants were expressed in *E. coli*. The encoding genes were in plasmids (pG-BsubpNBE) under control of a rhamnose inducible promoter, *rhaP*.[11, 49] bAChE and hAChE were expressed in *Pichia pastoris* as previously published and kindly provided by S. Vorlová as crude, nonlyophilized extracts for investigation.[50]

**Cell transformation, growth, and protein expression**: Competent *E. coli* DH5α cells were prepared by the transformation and storage solution method, and transformed according to a standard protocol.[11, 51] The transformed cells were plated on LB agar plates (containing 100 mg mL$^{-1}$ ampicillin).

For protein expression, LB-amp broth (5 mL) containing 100 mg mL$^{-1}$ ampicillin was inoculated with a single colony of recombinant DH5α and incubated overnight at 37 °C. The overnight culture was diluted 1:1000 in fresh LB-amp broth and cells were allowed to grow until an optical density at 600 nm ($OD_{600}$) of 0.5 – 0.7 was reached. Sterile rhamnose solution (200 g L$^{-1}$, 1% (v/v)) was then added to induce expression. Cells were incubated again for at least 8 h at 37 °C. Cells were collected by centrifugation, washed two times with sodium phosphate buffer (50 mM, pH 7.5) and resuspended in the same buffer for cell lysis by sonification. To remove cell debris, the solution was centrifuged again and the supernatant was lyophilized to yield the crude enzyme extract.

**Site-directed mutagenesis**: Site-directed mutagenesis was performed by using the "QuikChange" method (Stratagene, La Jolla, CA): Complementary primers bearing the nucleotides to be changed were used for PCR. Synthesis time was elongated to 8 min to ensure amplification of the complete plasmid. The PCR mixture was treated with *Dpn*I to digest the nonmethylated template DNA. Transformation and selection of recombinant cells were performed as described above.

**Synthesis of tertiary alcohol acetates**: Linalyl acetate (**1**) was obtained from Fluka (Buchs, Switzerland).

**(*R*/*S*)-2-Phenyl-3-butin-2-yl acetate (3)**: (*R*/*S*)-2-phenyl-3-butin-2-ol (25 g, 171 mmol) was dissolved in freshly distilled, dried tetrahydrofuran (300 mL). The solution was cooled on ice then BuLi (80 mL) in toluene (2.5 M, 200 mmol) was added dropwise over a period of 10 min. The mixture was stirred for another 15 min and freshly distilled acetyl chloride (15 mL, 211 mmol) was added. The ice bath was removed and the mixture was heated under reflux for 1 h. The solution was allowed to cool to ambient temperature and unconverted acetyl chloride was hydrolyzed by adding water (150 mL). The mixture was extracted three times with diethyl ether (300 mL) and the collected organic phases were dried with anhydrous $Na_2SO_4$ before the solvent was removed under a vacuum. Distillation (114 °C, 15 mbar) yielded the product as a colorless liquid (24.4 g, 130 mmol; 76%). $^1$H NMR (500.15 MHz, $CDCl_3$; tetramethylsilane (TMS) as standard): $\delta = 1.89$ (3H, s), 2.07 (3H, s), 2.80 (1H, s), 7.34 (1H), 7.36 (2H), 7.58 (2H) ppm. $^{13}$C NMR (125.76 MHz, $CDCl_3$; TMS as standard): $\delta = 21.71$, 32.05, 75.31, 75.56, 124.75, 124.84, 127.91, 128.33, 128.38, 142.10, 168.62 ppm.

**(*R*/*S*)-3-Methyl-1-pentin-3-yl acetate (2)**: Acetic anhydride (17 mL, 18.4 g, 180 mmol) was added dropwise to (*R*/*S*)-3-methyl-1-pentin-3-ol (17 mL, 14.8 g, 150 mmol) while the flask was cooled in an ice bath. Phosphorus pentoxide (50 mg) was added and the mixture was stirred for another 15 min, then the ice bath was removed and the mixture was stirred at ambient temperature for 16 h. The solution was washed twice with water (100 mL) and extracted twice with diethyl ether (100 mL). The organic layers were combined and washed with saturated $NaHCO_3$ solution until formation of $CO_2$ was no longer observed. The layers were again washed twice with water and dried over anhydrous $Na_2SO_4$ and then the solvent was removed. Flash chromatography on silica gel (petrol ether/ethyl acetate 4:1) yielded the product as a colorless liquid (17.65 g, 126 mmol, 84%). $^1$H NMR (500.15 MHz, $CDCl_3$; TMS as standard): $\delta = 1.03$ (3H, t, $J = 7.5$ Hz), 1.66 (3H, s), 1.85 (1H, m), 1.96 (1H, m), 2.03 (3H, s), 2.55 (1H, s) ppm. $^{13}$C NMR (125.76 MHz, $CDCl_3$; TMS as standard): $\delta = 8.40$, 21.89, 25.90, 34.67, 73.18, 75. 31, 83.75, 169.42 ppm.

**Biotransformation**: Reactions were either performed with a pH-stat system for conversion control (BsubpNBE) or in 2-mL reaction tubes for faster screening (CRL, AChEs).

pH-stat: An aqueous emulsion of the substrate ester (10 mM) was prepared with gum arabic (2% w/v) in an ultra turrax dispersing instrument. The emulsion (20 mL) was thermostated at 40 °C in the reaction chamber of the pH stat. The reaction was started by adding the enzyme (10 mg). The pH value was kept constant by automated titration with NaOH (0.1 M). At selected points of hydrolysis, determined by the amount of consumed NaOH, samples (200 μL) were withdrawn from the reaction mixture and extracted with toluene (250 μL). These samples were analyzed by GC separation on a chiral phase (Heptakis-(6-*O*-pentyl-2,3-di-*O*-methyl)-β-cyclodextrin in OV 1701, provided by Prof. König, University of Hamburg, Germany) and the carrier used was $H_2$ at 40 kPa.

In contrast to the other tested substrates, **3** showed significant autohydrolysis. This hydrolysis of **3** occurs by an $S_N1$-type mechanism[25] and shows only minor pH-dependence between pH 6.0 and 8.5, where a significant enzyme activity was observed. Lowest autohydrolysis rates were observed at near-neutral pH values. We decided to carry out measurements at pH 7.5, where autohydrolysis is only slightly higher than at pH 7.0 but significant enzyme activity is ensured. Enzymes were added in amounts sufficient to ensure 50% conversion within less than 20 min, which guaranteed that autohydrolysis contributed to less than 5% of the total conversion. For reactions with low catalytic activity and moderate or high enantioselectivity, however, autohydrolysis might reach similar levels as the enzymatic conversion of the disfavored enantiomer. As a result, the observed enantioselectivity would be slightly lower than the actual enantioselectivity of the enzymatic reaction.

  

**Molecular modeling**:

Hardware and software: Molecular modeling was performed on a Silicon Graphics Octane 2 workstation (SGI, Montain View, CA) with the Sybyl 6.1 program (Tripos, St. Louis, MO). The Tripos force field and Gasteiger-Hückel charges were used for all calculations. The partial charges of $His_{act}$ and the tetrahedral $Ser_{act.}$ – substrate complex were assigned as described previously.[52]

Structures: Experimentally determined X-ray structures of CRL (PDB entry 1LPM),[16] eeAChE (1C2B),[30] and hAChE (2CLJ)[31] were obtained from the Protein DataBank. A homology model of BsubpNBE DSM 402 was created by using the X-ray structures of the corresponding enzyme from the strain NRRL B8079 (1QE3, 1C7J, 1C7I).[53] The homology model for bAChE is based on the structure of AChE from *Torpedo californica* (1QIK, 1CFJ).[32] The homology models were computed by the Swiss-Model automated modeling service of GlaxoSmithKline (http://www.expasy.ch/swissmod/SWISS-MODEL.html).[54]

All solvent molecules represented in the PDB files were removed before substrate docking. Substrates were manually docked into the binding site of the enzymes to mimick the tetrahedral intermediate formed after the nucleophilic attack of the $Ser_{act.}$, which resembles the rate-limiting step of ester hydrolysis. The substrate was oriented with the oxyanion towards the oxyanion-hole residues and the protonated $N_{\varepsilon}$ atom embedded between the $O_{\gamma}$ and $O_{ester}$ atoms of the substrate.[52] The substituents of the substrate were oriented in the binding pocket to give minimal repulsive interactions with the protein structure.

**Molecular dynamics simulations**: The enzyme – substrate complex was optimized by energy minimization and subsequent 18-ps MD simulations (2 ps at 5 K, 2 ps at 30 K, 2 ps at 70 K, 12 ps at 100 K). The temperature coupling constant was adjusted to 10 fs. The non-bonded interaction cutoff was set to 8 Å, the dielectric constant to 1.0. The conformer structures were saved every 40 fs. Conformers of the last 2 ps were averaged and used for analysis. All minimizations and MD simulations were performed in vacuo with a constrained protein backbone.

To verify that results do not depend on the initial conformation or the simulation time, additional simulations with slightly different initial conformations and extended simulation times (100 ps) were performed. In all cases the system relaxed reproducibly to a similar conformation.

*The authors gratefully acknowledge Dr. Sandra Vorlová for providing recombinant* b*AChE and* h*AChE and Volker Nödinger for DNA sequencing. This work was supported by the Deutsche Forschungsgemeinschaft (Bo 1475/2 – 1) and the Bundesministerium für Bildung und Forschung (Project PTJ 31/0312702).*

[1] U. T. Bornscheuer, R. J. Kazlauskas, *Hydrolases in Organic Synthesis* 1st ed., Wiley-VCH, Weinheim, **1999**.
[2] a) A. Liese, K. Seelbach, C. Wandrey, *Industrial Biotransformations*, Wiley-VCH, Weinheim, **2001**; b) K. Faber, *Biotransformations in Organic Chemistry* 4th ed., Springer-Verlag, Berlin, **1999**.
[3] D. L. Ollis, E. Cheah, M. Cygler, B. Dijkstra, F. Frolow, S. M. Franken, M. Harel, S. J. Remington, I. Silman, J. Schrag, *Protein Eng.* **1992**, *5*, 197 – 211.
[4] a) P. Carter, J. Wells, *Nature* **1988**, *322*, 564 – 568; b) J. D. Schrag, Y. G. Li, S. Wu, M. Cygler, *Nature* **1991**, *351*, 761 – 764.
[5] a) M. Holmquist, *Chem. Phys. Lipids* **1998**, *93*, 57 – 66; b) T. Wagegg, M. M. Enzelberger, U. T. Bornscheuer, R. D. Schmid, *J. Biotechnol.* **1998**, *61*, 75 – 78.
[6] a) F. Björkling, J. Boutelje, Gatenbeck, K. Hult, T. Norin, *Tetrahedron Lett.* **1986**, *26*, 4957; b) G. Guanti, L. Banfi, E. Narisano, R. Riva, S. Thea, *Tetrahedron Lett.* **1986**, *27*, 4639 – 4642.
[7] N. Krebsfanger, K. Schierholz, U. T. Bornscheuer, *J. Biotechnol.* **1998**, *60*, 105 – 111.
[8] E. Keinan, E. K. Hafeli, K. K. Seth, L. R., *J. Am. Chem. Soc.* **1986**, *108*, 162.
[9] A. M. Klibanov, *Trends Biotechnol.* **1997**, *15*, 97 – 101.
[10] U. H. Kahlow, R. D. Schmid, J. Pleiss, *Protein Sci.* **2001**, *10*, 1942 – 1952.
[11] E. Henke, U. T. Bornscheuer, *Biol. Chem.* **1999**, *380*, 1029 – 1033.
[12] K. E. Jaeger, T. Eggert, A. Eipper, M. T. Reetz, *Appl. Microbiol. Biotechnol.* **2001**, *55*, 519 – 530.
[13] D. Zha, S. Wilensek, M. Hermes, K. E. Jaeger, M. T. Reetz, *Chem. Commun.* **2001**, *24*, 2664 – 2665.
[14] a) F. Manetti, D. Mileto, F. Corelli, S. Soro, C. Palocci, E. Cernia, I. D'Acquarica, M. Lotti, L. Alberghina, M. Botta, *Biochim. Biophys. Acta* **2000**, *1543*, 146 – 158; b) D. Rotticci, J. C. Rotticci-Mulder, S. Denman, T. Norin, K. Hult, *ChemBioChem* **2001**, *2*, 766 – 770.
[15] H. Scheib, J. Pleiss, P. Stadler, A. Kovac, A. P. Potthoff, L. Haalck, F. Spener, F. Paltauf, R. D. Schmid, *Protein Eng.* **1998**, *11*, 675 – 682.
[16] M. Cygler, P. Grochulski, R. J. Kazlauskas, J. D. Schrag, F. Bouthillier, B. Rubin, A. N. Serreqi, A. K. Gupta, *J. Am. Chem. Soc.* **1994**, *116*, 3180.
[17] R. J. Kazlauskas, A. N. E. Weissfloch, A. T. Rappaport, L. A. Cuccia, *J. Org. Chem.* **1991**, *56*, 2656 – 2665.
[18] a) F. Carriere, E. Rogalska, C. Cudrey, F. Ferrato, R. Laugier, R. Verger, *Bioorg. Med. Chem.* **1997**, *5*, 429 – 435; b) A. N. E. Weissfloch, R. J. Kazlauskas, *J. Org. Chem.* **1995**, *60*, 6959 – 6969.
[19] H. Scheib, J. Pleiss, A. Kovac, F. Paltauf, R. D. Schmid, *Protein Sci.* **1999**, *8*, 215 – 221.
[20] T. Schulz, J. Pleiss, R. D. Schmid, *Protein Sci.* **2000**, *9*, 1053 – 1062.
[21] S. Raza, L. Fransson, K. Hult, *Protein Sci.* **2001**, *10*, 329 – 338.
[22] a) E. J. Corey, A. Guzman-Perez, *Angew. Chem.* **1998**, *110*, 402 – 415; *Angew. Chem. Int. Ed.* **1998**, *37*, 388 – 401; b) J. Christoffers, A. Mann, *Angew. Chem.* **2001**, *113*, 4725 – 4732; *Angew. Chem. Int. Ed.* **2001**, *40*, 4591 – 4597.
[23] R. D. Schmid, R. Verger, *Angew. Chem.* **1998**, *110*, 1694 – 1720, *Angew. Chem. Int. Ed.* **1998**, *37*, 1608 – 1633.
[24] a) A. Schlacher, T. Stanzer, I. Osprian, M. Mischitz, E. Klingsbichel, K. Faber, H. Schwab, *J. Biotechnol.* **1998**, *62*, 47 – 54; b) D. O'Hagan, N. A. Zaidi, *J. Chem. Soc. Perkin Trans. 1* **1992**, *8*, 947 – 949.
[25] D. O'Hagan, N. A. Zaidi, *Tetrahedron: Asymmetry* **1994**, *5*, 1111 – 1118.
[26] E. Henke, J. Pleiss, U. T. Bornscheuer, *Angew. Chem.* **114**, 3138 – 3340; *Angew. Chem. Int. Ed.* **2002**, *41*, 3211 – 3213.
[27] J. Pleiss, M. Fischer, M. Peiker, C. Thiele, R.-D. Schmid, *J. Mol. Catal. B: Enzym.* **2000**, *10*, 491 – 508.
[28] a) A. Ordentlich, D. Barak, C. Kronman, N. Ariel, Y. Segall, B. Velan, A. Shafferman, *J. Biol. Chem.* **1998**, *273*, 19509 – 19517; b) A. K. Whiting, W. L. Peticolas, *Biochemistry* **1994**, *33*, 552 – 561; c) P. Bryan, M. W. Pantoliano, S. G. Quill, H. Y. Hsiao, T. Poulos, *Proc. Natl. Acad. Sci. U.S.A.* **1986**, *83*, 3743 – 3745.
[29] Y. Hotta, S. Ezaki, H. Atomi, T. Imanaka, *Appl. Environ. Microbiol.* **2002**, *68*, 3925 – 3931.
[30] Y. Bourne, J. Grassi, P. E. Bougis, P. Marchot, *J. Biol. Chem.* **1999**, *274*, 30370 – 30376.
[31] C. E. Felder, S. A. Botti, S. Lifson, I. Silman, J. L. Sussman, *J. Mol. Graphics Modell.* **1997**, *15*, 318 – 327, 335 – 317.
[32] C. B. Millard, G. Kryger, A. Ordentlich, H. M. Greenblatt, M. Harel, M. L. Raves, Y. Segall, D. Barak, A. Shafferman, I. Silman, J. L. Sussman, *Biochemistry* **1999**, *38*, 7032 – 7039.
[33] C. Chen, Y. Fujimoto, G. Girdaukas, C. J. Sih, *J. Am. Chem. Soc.* **1982**, *104*, 7294 – 7299.
[34] T. Schulz, R. D. Schmid, J. Pleiss, *J. Mol. Model.* **2001**, *7*, 265 – 270.
[35] a) F. Haeffner, T. Norin, K. Hult, *Biophys. J.* **1998**, *74*, 1251 – 1262; b) J. Ottosson, J. C. Rotticci-Mulder, D. Rotticci, K. Hult, *Protein Sci.* **2001**, *10*, 1769 – 1774.
[36] D. Farb, W. P. Jencks, *Arch. Biochem. Biophys.* **1980**, *203*, 214 – 226.
[37] a) D. Seebach, M. Eberle, *Chimia* **1986**, *40*, 315 – 318; b) W. Junge, E. Heymann, *Eur. J. Biochem.* **1979**, *95*, 519 – 525; c) E. Heymann, W. Junge, *Eur. J. Biochem.* **1979**, *95*, 509 – 518.
[38] A. Musidlowska, S. Lange, U. T. Bornscheuer, *Angew. Chem.* **2001**, *113*, 2934 – 2936; *Angew. Chem. Int. Ed.* **2001**, *40*, 2851 – 2853.

  

[39] a) T. Katsuki, K. B. Sharpless, *J. Am. Chem. Soc.* **1980**, *102*, 5974 – 5976; b) L. D. L. Lu, R. A. Johnson, M. G. Finn, K. B. Sharpless, *J. Org. Chem.* **1984**, *49*, 728 – 731.
[40] R. C. Milton, S. C. Milton, S. B. Kent, *Science* **1992**, *256*, 1445 – 1448.
[41] a) M. Chen-Goodspeed, M. A. Sogorb, F. Wu, S. B. Hong, F. M. Raushel, *Biochemistry* **2001**, *40*, 1325 – 1331; b) M. Chen-Goodspeed, M. A. Sogorb, F. Wu, F. M. Raushel, *Biochemistry* **2001**, *40*, 1332 – 1339.
[42] H. K. W. Kallwass, J. K. Hogan, E. L. A. Macfarlane, V. Martichonok, W. Parris, C. M. Kay, M. Gold, J. B. Jones, *J. Am. Chem. Soc.* **1992**, *114*, 10 704 – 10 710.
[43] A. E. Tripp, D. S. Burdette, J. G. Zeikus, R. S. Phillips, *J. Am. Chem. Soc.* **1998**, *120*, 5137 – 5141.
[44] O. May, P. T. Nguyen, F. H. Arnold, *Nat. Biotechnol.* **2000**, *18*, 317 – 320.
[45] a) L. Zidek, M. V. Novotny, M. J. Stone, *Nat. Struct. Biol.* **1999**, *6*, 1118 – 1121; b) J. L. Radkiewicz, H. Zipse, S. Clarke, K. N. Houk, *J. Am. Chem. Soc.* **2001**, *123*, 3499 – 3506; c) M. J. Osborne, J. Schnell, S. J. Benkovic, H. J. Dyson, P. E. Wright, *Biochemistry* **2001**, *40*, 9846 – 9859.
[46] G. C. d. Q. Robin, C. Claudianos, R. J. Russell, J. G. Oakeshott, *J. Mol. Evol.* **2000**, *51*, 149 – 160.
[47] P. Lebaron, J. F. Ghiglione, C. Fajon, N. Batailler, P. Normand, *FEMS Microbiol. Lett.* **1998**, *160*, 137 – 143.
[48] a) F. Kunst, N. Ogasawara, et al., *Nature* **1997**, *390*, 249 – 256; b) J. Zock, C. Cantwell, J. Swartling, R. Hodges, T. Pohl, K. Sutton, P. Rosteck, D. McGilvray, S. Queener, *Gene* **1994**, *151*, 37 – 43.
[49] I. Pelletier, J. Altenbuchner, *Microbiology* **1995**, *141*, 459 – 468.
[50] a) S. Minning, A. Serrano, P. Ferrer, C. Sola, R. D. Schmid, F. Valero, *J. Biotechnol.* **2001**, *86*, 59 – 70; b) S. Vorlová, J. Schmitt, R. D. Schmid, *Biochim. Biophys. Acta* **2003**, submitted.
[51] J. Sambrook, E. F. Fritsch, T. Maniatis, *Molecular Cloning: A Laboratory Manual*, Cold Spring Harbor Laboratory Press, Cold Spring Harbor, N. Y., **1989**.
[52] H.-C. Holzwarth, J. Pleiss, R.-D. Schmid, *J. Mol. Catal. B: Enzym.* **1997**, *3*, 73 – 82.
[53] B. Spiller, A. Gershenson, F. H. Arnold, R. C. Stevens, *Proc. Natl. Acad. Sci. U.S.A.* **1999**, *96*, 12 305 – 12 310.
[54] N. Guex, M. C. Peitsch, *Electrophoresis* **1997**, *18*, 2714 – 2723.

Received: October 25, 2002
Revised version: March 3, 2003 [F 518]

  